Properties of Marginally-Stable Collisionless Drift-Universal Modes with Application to the W-II Stellarator

J.E. McCune and K.U. von Hagenow

IPP 6/85

April 1970

INSTITUT FÜR PLASMAPHYSIK

GARCHING BEI MÜNCHEN

INSTITUT FÜR PLASMAPHYSIK

GARCHING BEI MÜNCHEN

Properties of Marginally-Stable Collisionless Drift-Universal Modes with Application to the W-II Stellarator

J.E. McCune and K.U. von Hagenow

IPP 6/85

April 1970

Die nachstehende Arbeit wurde im Rahmen des Vertrages zwischen dem Institut für Plasmaphysik GmbH und der Europäischen Atomgemeinschaft über die Zusammenarbeit auf dem Gebiete der Plasmaphysik durchgeführt.

IPP 6/85 J.E. McCune
K.U. von Hagenow

Properties of Marginally-Stable Collisionless Drift-Universal Modes with Application to the W-II Stellarator

April, 1970 (in English)

ABSTRACT:

The marginal-stability properties of a class of collisionless drift-universal plasma modes are studied numerically and analytically. The familiar "slab" model of plasma equilibria with gradients perpendicular to $\underline{B}$ is employed, and both hydrogen and barium plasmas are treated. This study extends earlier work in that specific information is provided which enables one to decide whether or not a given mode is unstable in a given machine; possible application to the Wendelstein (WII) experiment at low densities is discussed. Analytic formulas for the properties of the marginally stable modes are developed. The marginally stable modes divide roughly into three regimes: small m-number modes with sufficiently long parallel wave lengths first become unstable at relatively low densities ("low-density branch") and are then stabilized again as the density is increased ("high-density branch"); large m-number modes, by contrast, possess a critical parallel wave length which decreases monotonically with increasing density. Departure from quasi-neutrality is very important for these higher m-number waves; their frequencies at threshold are very small and inversely proportional to the critical parallel wave length.

Acknowledgements

A major portion of this work was performed during the summer of 1969 at the Institut für Plasmaphysik. The work of one of the authors (J.E.M.) was also supported in part, at M.I.T., by the United States Air Force Office of Scientific Research under Grant No. AFOSR 69-1697. The authors wish to express their appreciation to Mr. R.L. McCroy of the M.I.T.Department of Nuclear Engineering for obtaining the numerical results given in Fig.3.

I. Introduction

Low frequency ($\omega < \Omega_i$) drift instabilities in nonuniform plasmas have been studied extensively over the past decade, with a wide range of plasma conditions having been considered. A great variety of destabilizing effects for these modes has been identified. Plasma equilibria with "low-ß" as well as "moderate-ß" have been treated, and both the collision-dominated and "collisionless" regimes considered. Nonuniformity of the plasma perpendicular tothe magnetic field provides the inherent source of free energy available for the instability. Such nonuniformities have been simulated theoretically in a number of ways, ranging from a relatively simple plane-geometry model to treatment in general magnetic field configurations. Even the simplest of these models has not been fully exploited as yet; in this report we offer specific information obtained from the "slab model" (see Section II) which is intended to aid in answering the question of whether a specific "drift--universal" mode is or is not unstable in a specific machine. In many interesting situations the drift modes have properties which differ substantially from those obtained by approximate analyses. Of course, the results are restricted by the model used; it is hoped, however, that they will provide a guide and stimulus for future investigations.

The vast literature on drift instabilities reflects their enormous variety; we make no attempt to survey the literature completely here. In the collisional regime destabilizing effects include ion inertia, current along the field, and electron-ion collisions. An extensive (but not exhaustive!) survey of the theory of "drift-dissipative" (collisional) instabilities has been given by Rukhadze and Silin [1], [2]. Experimental identification of these modes in Q-machines has been made by several investigators. (See, for example, Refs. [3], [4], [5].)

In this report we shall be concerned exclusively with unstable drift modes in the collisionless regime. Moreover, because of the application we have in mind, we shall limit our attention to the "low-ß" regime and make the usual electrostatic approximation for the perturbed electric field.

In the collisionless regime the mechanism for tapping the available free energy involves resonant interaction of the electron motion along the lines with the perturbed electric field. In the unstable regime a net exchange of energy from the resonant particles to the waves is affected by the perturbation $\underline{E} \times \underline{B}$ motion which moves particles across the field from higher to lower density regions in just the proper phase to provide inverse electron Landau damping. In many regimes of interest a competing stabilizing effect is provided by ion Landau damping. More detailed description of the physical mechanisms of drift instabilities may be found, for example, in Refs. [6] and [7].

Because of the stabilizing effect of ion Landau damping, drift instabilities are not expected to occur in plasma configurations which are too "short" along the magnetic field $\underline{B}$ [8]. "Drift-universal" instabilities with $k_\perp a_i \gtrsim 1$, for example, are not stabilized by "minimum-B" configurations, and it is believed, therefore, that it is this "length effect" which accounts for the absence of observation of drift-universal modes (so far) in mirror machines.

Toroidal machines, on the other hand, may have effective "connection-lengths" along $\underline{B}$ which are very long, and it seems probable that drift-universal instabilities will arise in such devices (Section III). Of course, curvature and shear effects, not considered here, will modify our results, but complete stabilization of the many potentially unstable modes identified seems unlikely.

In Section II we discuss the theoretical models available for study of drift instabilities, and include a discussion of the frequently-used "local approximation". In Section III the properties at marginal stability of drift-universal modes, driven by density gradients alone, are discussed. Numerical results are obtained, using an efficient program developed by Callen. This work differentiates itself from earlier studies in that the effects of finite density (more precisely, departure from quasi-neutrality) are emphasized and the properties of modes with $k_\perp a_i$ far from the "most unstable" value emphasized by Krall and Rosenbluth are determined. Both hydrogen (H^+) and Barium (Ba^+) plasmas are studied, and possible application to the Wendelstein (WII) experiment discussed.

Values of growth rates and real frequencies will be given in a subsequent report for a variety of modes in the unstable regimes defined in this study.

II. Theoretical Models for Drift Instabilities

The majority of the original work on collisionless drift modes employs a plane-geometry configuration ("slab model") with the plasma equilibrium varying in a single direction perpendicular to $\underline{B}$ (cf [8], [9], [10] and [11]). The most extensive discussions of the salient features of this type of equilibria are provided by Krall and Rosenbluth [10] and Callen [11]. In the usual slab model the magnetic lines are straight with ∇B included, while magnetic field curvature is simulated (only qualitatively ([12], [13])!) by an effective acceleration (parallel or antiparallel to the pressure gradient). To a certain extent, magnetic field shear can also be included ([10], [14]). While it is clear that is a long step from a plane-

geometry model to a toroidal configuration, the slab model has the advantage that particle-wave resonances combined with the important finite Larmor radius effects can be included with relative ease. Indeed, finite Larmor radius effects are included "exactly" -- within the model. In the work reported here, we make extensive use of this model; the purpose of the present Section is to indicate some of its limitations and to note briefly the work that has been undertaken to overcome these restrictions.

Politzer [15], as part of his theoretical and experimental study of collisionless drift waves, has analyzed the problem in a cylindrical magnetic field geometry using a modified drift-kinetic approach. He includes first-order finite Larmor-radius corrections to the drift velocity and particle- (versus guiding center-) density for the ions to obtain the 'universal' instability. His treatment includes (in principle) arbitrary steady-state electric field gradients and such effects as the centrifugal and Coriolis forces associated with the $\underset{\sim}{E}_o \times \underset{\sim}{B}_o$ rotation of the particles. Thus, on the one hand, he can indicate the relative importance of these latter effects (which are absent in the slab model) but on the other hand cannot include, at least in a simple way, higher-order finite Larmor radius effects. He also provides, from his analysis, a means of estimating the appropriate relation between the "perpendicular wave number" of the slab model and the azimuthal mode number in cylindrical geometry. Politzer's work provides an important intermediate step between the plane-geometry model and the analysis in general magnetic field configurations.

Rutherford and Frieman [16] have set up the general linearized electrostatic problem for low frequency modes by deriving the appropriate integral equation for the disturbed potential in a general magnetic field configuration. They exploit their result in axially-symmetric toroidal configurations, obtaining the

drift-universal modes (and other expected instabilities as well) in certain familiar limits, for example, in the regime for which the phase speed of the modes along $\underline{B}$ is intermediate between the electron and ion thermal speeds. Much more work is required in using this elegang tool to evaluate the strengths and weaknesses of the slab model. For example, it is not clear at this writing how we can obtain solutions of the integral equation in regimes other than those treated by Rutherford and Frieman. Yet, as we shall see below, the "slab model" predicts unstable modes of interest in regimes quite foreign to the limits studied in Ref. [16].

Even in the relatively simple slab model the actual equation for the perturbed potential is an integral equation. This can be reduced to a differential equation by expanding the general operator in powers of the ratio of the ion Larmor radius, a_i, to the shortest of the scale lengths, L_p, of the plasma equilibrium gradients [8]. (In the low-ß limit, in the absence of curvature, the most important scale length is that associated with the pressure gradient). If one is willing to drop terms of higher order than $(a_i/L_p)^2$ the result is a second-order ordinary differential equation for the perturbed plasma potential ([8], [10], [11]) which can be treated by relatively standard WKB methods. When magnetic field shear is present, WKB analysis is essential to determine the existence and properties of eigenmodes ([10], [14], [17]); in the absence of shear the WKB analysis has been used primarily (to date) to justify the so-called "local approximation" to the dispersion relation determining the eigenfrequencies of modes localized around the maximum of the logarithmic steady-state pressure (or density) gradient. It is this "local approximation" which we will use to obtain explicit results in Section III.

To understand the local approximation within the slab model let us imagine that the equation for the perturbed potential has been reduced to the form ($\tilde{\phi} = \phi(x) \exp\{-i\omega t + ik_y v_y + ik_z v_z\}$):

$$\frac{d^2\phi}{dx^2} = - D(\omega, \underline{k}; x)\,\phi(x) \qquad (2.1)$$

where the gradients in the plasma are in the x-direction, $\underline{k} = (0, k_y, k_z)$ and $\underline{B} = (0, 0, B_z(x))$. (Let us assume no shear for the purposes of our present discussion.) In that case, $D(\omega, \underline{k}; x)$ depends on x primarily through the pressure- (or density-) gradient (because of our low-ß assumption) and we might expect drift modes, if they occur, to be "localized" near the point of maximum $\left|\frac{1}{n_0}\frac{dn_0}{dx}\right|$. We then look for frequencies ω such that $Re\,[D(\omega, x_0)] > 0$, $Re\,[\partial^2 D/\partial x^2]_{x=x_0} \lesssim 0$, where x_0 is defined by $(\partial D/\partial x)_\omega = 0$. Then, if there exist nearby points $x_1(\omega)$ and $x_2(\omega)$ (they will, in general, be complex) at which $D(x_1, \omega) = D(x_2, \omega) = 0$ we can expect to find solutions of a standing wave nature near x_0 which die out spatially as $|x - x_0|$ exceeds $|x_1 - x_2|$. To be explicit, if we assume $|x_1 - x_2|/L_p \ll 1$, we can expand $D(\omega, x)$ about x_0 and find

$$x_2 - x_1 \cong 2\sqrt{-2\,D(\omega, x_0)/D_{xx}(\omega, x_0)}\,. \qquad (2.2)$$

This result, when evalutated, provides a measure of the scale length over which $\phi(x)$ changes appreciably.

Applying the usual phase-integral condition for the ℓth eigenmode of (2.1), under the conditions outlined above, we obtain the "dispersion relation"

$$D(\omega^{(\ell)}, x_0) \cong (2\ell+1)\sqrt{-D_{xx}(\omega^{(\ell)}, x_0)/2} \qquad (2.3)$$

for the corresponding eigenfrequencies $\omega^{(\ell)}$. Now if we define ω_0 such that $D(\omega_0, x_0) = 0$ and assume $\omega^{(\ell)} - \omega_0 \equiv \delta\omega^{(\ell)} \ll \omega_0$ we obtain the expression (cf., Ref. [8])

$$\frac{\delta\omega^{(\ell)}}{\omega_0} \cong (\ell + \tfrac{1}{2})\,\frac{\sqrt{-2\,D_{xx}(\omega_0, x_0)}}{\omega_0 \frac{\partial D}{\partial \omega}(\omega_0, x_0)} \qquad (2.4)$$

Then, if we can determine ω_o , we can, within the present approximations, determine the eigenfrequencies by correcting ω_o according to (2.4). If $\delta\omega^{(2)}/\omega_o \ll 1$, we can often be satisfied with the approximation ω_o itself. As already stated, this is determined by

$$D(\omega_o, \underline{K}; x_o) = 0 \tag{2.5}$$

which, in this sense, replaces (2.3) as the dispersion relation for the modes we seek. This is the "local approximation" to the dispersion relation, which we use in the remainder of this report (see also, Refs. [8], [10] and [11]). Formally, of course, (2.5) is the same result as that obtained by simply treating $\tilde{\phi}$ to be independent of x near x_o , a fact which has occasionally led to some misunderstanding of the meaning of the local approximation. In fact, the localized eigenmode must change <u>rapidly</u> in x , on a scale much smaller than L_p, for the above analysis to hold, i.e., we must have $|x_1 - x_2|/L_p \ll 1$.

It turns out that $D(\omega, x)$, in the approximation appropriate to Eq.(2.1), can be written in the form

$$D(\omega, x) = \frac{-k^2\lambda_{Di}^2 + H(\omega, \underline{K}, \cdots x)}{\lambda_{Di}^2 + q(\omega, \underline{K}, x)a_i^2} \tag{2.6}$$

where $q(\omega, \underline{K}, x)$ is a complex quantity of order unity, $k^2 \equiv K_y^2 + K_z^2$, and λ_{Di} is the local ion Debye length. $H(\omega, \underline{K}, \cdots x)$ is written out in the next Section (Eq.(3.1)). Working out the required derivatives of $D(\omega, x)$ we find typically in the drift wave regime

$$\frac{|x_1 - x_2|}{L_p} \simeq \frac{|\lambda_{Di}^2 + q a_i^2|^{1/4}}{L_p^{1/2}(k^2\lambda_{Di}^2 + \alpha)^{1/4}} \tag{2.7}$$

and

$$\frac{\delta\omega^{(\ell)}}{\omega_0} \cong (\ell+\tfrac{1}{2}) \frac{|\lambda_{Di}^2 + q\, a_i^2|^{1/2}}{L_p (K^2\lambda_{Di}^2 + \alpha)^{1/2}} \qquad (2.8)$$

where α is of order unity. Thus, provided the microscopic lengths, a_i and λ_{Di}, remain sufficiently small compared to L_p, the local approximation is justified (for moderate ℓ) over the entire density regime, including the "quasi-neutral limit",

This latter statement, however, requires careful interpretation. For direct application to experiment (cf. Section III) the quantities λ_{Di}/a_i and a_i/L_p are fixed, while $K \approx K_t$ increases roughly proportional to the azimuthal mode number, m. In this case, high m-number modes see the plasma as a "low-density" one, i.e. $K\lambda_{Di} \to \infty$. Looking at the problem this way leads to the conclusion that the local approximation is best satisfied in the low density limit. Clearly, by contrast, if we understand the low density limit to mean $\lambda_{Di}/a_i \to \infty$ with $K\lambda_{Di}$ fixed, then the local approximation will break down (see Eqs. (2.) and (2.8)) unless $a_i/L_p \to 0$. Fortunately, this is not the limit of interest (see Section III).

Finally, we point out that the reference frame used in the slab model is not the rest frame for either the ions, the electrons or the plasma as a whole. Rather, it is the field-free frame ($\underline{E}_0$(local) = 0). Hence, as is well known, the real part of the frequency must generally be Doppler shifted for comparison with experiment. In particular, the velocity, (perpendicular to $\underline{B}_0$ and ∇n_0) of the slab-model-frame with respect to the rest frame for the plasma as a whole is approximately the electron diamagnetic velocity when the temperatures of the ions and electrons are equal.

III. Threshold Properties

In this Section we consider the properties of 'drift-universal' modes in the marginally stable state, using the slab model of the plasma equilibrium. The specific results reported here are for nonuniform equilibria described by the steady-state distribution functions appropriate to the slab model ([8], [10], [11])

$$f_s^0 = f_s^0 \left(v_\perp^2,\ v_z,\ x + \frac{v_y}{\Omega_s} \right)$$

$$\cong \left[1 - \epsilon' \left(x + \frac{v_y}{\Omega_s} - x_0 \right) \right] \frac{1}{\pi^{3/2} \alpha_s^3}\ e^{-v^2/\alpha_s^2}$$

where $s = i, e$, the geometry is that described below Eq.(2.1), and we have neglected $[dB/dx]/B$ compared to $n_0^{-1}[dn_0/dx]_{x=x_0}$ because of our assumption of low ß. Clearly, these distributions represent a locally constant-temperature plasma ($\alpha_s^2 = 2kT_s/m_s$) with a weak density gradient in the x-direction, measured locally by $\epsilon' \approx L_p^{-1}$. In the following, we shall identify x_0 with the "x_0" defined in Section II; x_0 is then located near the maximum of $n_0^{-1}|dn_0/dx|$.

The weak dependence of the f_s on the guiding center variables, $x + \frac{v_y}{\Omega_s}$ introduces, of course, the usual average diagmagnetic "drift velocities" in the y-direction for each species, which are necessary to balance the pressure gradients. It also introduces a velocity-space anisotropy which, as it turns out, brings in odd-order derivative terms in the equation for $\phi(x)$ (cf., Eq.(2.1) and Ref. [11]). However, these terms turn out to be unimportant within the range of applicability of the slab model [11] and we do not discuss them further here.

While, in the interest of simplicity, we limit our attention in this report to the case described above (density gradient only) the computer programs used, which are adapted from

Ref. [11], are capable of including temperature anisotropies, gradients in any of the temperatures as well as the density, currents along $\underline{B}$, and an acceleration field in the x-direction (to simulate magnetic curvature). "Loss cone" effects can also be simulated.

We now adopt the "local approximation" described in Section II, determining ω_o instead of the actual eigenfrequencies $\omega^{(\ell)}$ (see Eq.(2.4)). Our approximate dispersion relation then becomes Eq.(2.5), which, for the f_s^o given above, reduces to ([8], [10]):

$$k^2\lambda_{Di}^2 = -\left(1+\frac{1}{\Theta}\right) - \beta_i \frac{\omega + \frac{\omega_*}{\Theta}}{k_z \alpha_i} Z\left(\frac{\omega}{k_z\alpha_i}\right) - \beta_e \Theta\sqrt{\delta}\,\frac{\omega-\omega_*}{k_z\alpha_i} Z\left(\frac{\omega}{k_z\alpha_i}\sqrt{\frac{\delta}{\Theta}}\right)$$

$$\equiv H(\omega, \underline{k}; \cdots x_o) \qquad (3.1)$$

where we have assumed $k_z > 0$, and dropped the subscript "o" on ω. $Z(w)$ is the familiar plasma dispersion function [18] and we have introduced the additional notation, $\Theta = T_e/T_i$, $a_{i,e} = \frac{\alpha_{i,e}}{\Omega_{i,e}}$,

$$\delta = m_e/m_i, \quad \beta_{i,e} = \beta(b_{i,e}), \quad \beta_s \equiv e^{-b_s} I_o(b_s), \quad \omega_* \equiv k_y V_{de} = -\frac{k_y \alpha_e^2}{2\Omega_e}\epsilon'$$

The density-dependent parameters are evaluated at x_o: $\epsilon' = -\frac{1}{n_o}\frac{dn_o}{dx}\Big|_{x=x_o}$, $\lambda_{Di}^2 = \frac{\alpha_i^2}{2\omega_{pi}^2(x_o)}$. ω_{pi} is the ion plasma frequency (at x_o) and we have assumed $|\omega| \ll \Omega_i$. Solutions of (3.1) with $\mathrm{Im}(\omega) > 0$ imply instability. Note that $\beta_{i,e} \lesssim 1$.

For a given value of density (λ_{Di}) there is a maximum value of k_z, above which drift waves are stabilized by ion Landau damping; thus, as noted earlier, drift wave instabilities are not expected to occur for plasma configurations which do not admit sufficiently long wave lengths in the direction along $\underline{B}$. Similarly, <u>for given</u> k_z, there is a minimum plasma density below which there are insufficient particles to provide the collective motion required to

support the wave. Hence, for each $k_y a_i$, we can determine a threshold curve for instability in the $(k^2 \lambda_{Di}^2, k_z/\epsilon')$ plane. Krall und Rosenbluth [10] use this fact to determine a formula for $(k_z)^{max}$ versus $k^2 \lambda_{Di}^2$ which provides a sufficient condition for stability against these modes. In essence, their result is obtained by maximizing the threshold value of k_z/ϵ' versus $k_y a_i$ at each density; the success of their formula in the sense for which it is intended will be apparent in what follows (Figs. 2, 2a, 2b).

The actual threshold conditions for onset of instability according to (3.1) are, however, strong functions of $k_y a_i$ (or b_i) in interesting parameter ranges. For application to particular plasma experiments what is actually needed is to determine the conditions for onset of instability of a particular set of modes (e.g., particular values of $k_y a_i$); usually the modes of interest are much "more stable" (in the sense that much higher densities or longer parallel wave lengths are required) than an estimate based on Krall and Rosenbluth's sufficient condition would indicate.

In addition, it is of considerable interest to determine the frequency of the mode at the onset of instability. It turns out that a simple analytical formula (3.3) can be given for this frequency, which, for a wide range of values of $k_y a_i$, is accurate (at threshold) over the full range of k_z's which admit instability. More importantly, the phase speed along $\underline{B}$, at onset, is often comparable to or even less than, the ion thermal speed and the frequently -used approximation, $\omega/k_z \alpha_i \gg 1$, is not applicable in this regime. This fact can also be observed in the results of Krall and Rosenbluth [10], and may, among other effects, have significant implications with regard to the amount of magnetic shear required to stabilize a given drift mode.

To determine the general threshold properties of the unstable modes described by (3.1) we proceed as in Ref. [11], and first look for the zeros of Im H(+ i0) . Introducing $\hat{z} \equiv \frac{\omega}{\Omega_i} = X + iY$, $\chi_* \equiv \omega_*/\Omega_i = \Theta \frac{k_y a_i}{2} \epsilon' a_i$, $K = k_\perp a_i$, we have for $\hat{z} = X + i0$

$$0 = \beta_i \left(X + \frac{\chi_*}{\Theta}\right) e^{-X^2/K^2} + \frac{\beta_e}{\Theta^{3/2}} (X - \chi_*) \sqrt{\delta}\, e^{-\frac{\delta}{\Theta}\frac{X^2}{K^2}}$$

which can be written

$$K^2 = \frac{X^2 (1 - \delta/\Theta)}{\ln(\Theta^{1/2}\beta_i/\sqrt{\delta}\beta_e) - \ln\left(\frac{\chi_* - X}{\chi_* + \Theta X}\right)} \qquad (3.2)$$

We assume for definiteness $\omega_* > 0$ (density decreasing with the spatial coordinate x). Then, general consideration of a Nyquist diagram for $H(\omega + i0)$ shows that marginally stable solutions of (3.1), if any, exist in the range $0 < X < \chi_*$. On the other hand, (3.2) shows that $K^2(X)$ corresponding to Im $H(\omega + i0) = 0$ increases from zero quadratically with X and then is cut off sharply at $X = \chi_*$, with a maximum of K^2 near χ_*. (Above this maximum K , drift waves are ion Landau-damped at any frequency.) It is not difficult to show that $K^{max} < \chi_*$ for Θ near unity, while $K^{max} < \Theta^{1/2}\chi_*$ for large Θ.

The properties of (3.2) described above indicate that for any $K < K^{max}$ there are two solutions X(K) of Im $H(\omega + i0) = 0$ in the range $0 < X < \chi_*$. Usually, only <u>one</u> of these solutions will also satisfy the real part of (2.1), and, in fact, this will be the smaller of the two frequencies. For $X \ll \chi_*$ and Θ not too large (3.2) can be solved analytically, since then $\ln[(\chi_* - X)/(\chi_* + \Theta X)] \cong -(1+\Theta)X/\chi_*$; the result is, to a good approximation,

$$\frac{\omega}{k_\perp \Omega_i} \equiv \frac{X}{K} \cong \sqrt{\ln(\Theta^{1/2}\beta_i/\sqrt{\delta}\beta_e)}\; + \frac{1+\Theta}{2}\frac{K}{\chi_*}\, i \quad \text{(threshold)} \qquad (3.3)$$

In the last expression we have assumed $\delta/\theta \ll 1$. The condition for the validity of (3.3) is essentially that the first term be large compared to the second; for $k_y a_i \gtrsim 0.4$ and θ not too large our numerical calculations show that this is well fulfilled at threshold over the <u>entire</u> "unstable range" of k_z/ϵ' (cf. Fig. 1). Even for smaller $k_y a_i$, Eq.(3.3) is useful on what we call the "low density branch" of the small-$k_y a_i$ marginally stable modes. We note that in the region of validity of (3.3) the threshold phase speed, along <u>B</u>, is nearly a constant, depending on $k_y a_i$, θ, and the mass ratio, and is generally <u>not</u> large compared to unity (Figs. 1 - 1b). Nevertheless, in cases where (3.3) yields $\sqrt{\theta/\delta} \gg \omega/k_z \alpha_i \gtrsim 2$ an alternative expression for (3,3) should hold, provided it is also much less than ω_*:

$$\omega(\text{threshold}) \cong \frac{\omega_*}{\left(1+\frac{1}{\theta}\right) + k^2\lambda_{D_i}^2 - \beta_i} \qquad (3.4)$$

The two conditions mentioned above for the overlap of (3.4) and (3.3) can be fulfilled for a proton plasma only if $\theta^{1/2}\beta_i \cong 1$ and hence require (from (3.4)) $k^2\lambda_{D_i}^2 \gg 1$ and/or $\theta \gg 1$. For a $\theta = 1$ proton plasma (3.4) holds, at best, only on the "low-density branch" of the stability curves for $k_y a_i \lesssim 0.4$ and is only a fair approximation for larger $k_y a_i$ (see below).

Numerical results for the frequency at threshold for a wide range of values of $k_y a_i$ were obtained using the programs developed in Ref. 11. Threse are presented for $T_e = T_i$ ($\theta = 1$) in Fig. 1 for a proton plasma. Comparisons with Eq.(3.3), shown in Fig. 1, verify its usefulness. Also, because it is so frequently used as an estimate of the drift mode frequency, the <u>quasi-neutral limit</u> ($k\lambda_{D_i} \to 0$) of (3.4) is shown on Fig. 1 for reference. Clearly, for modes with $k_y a_i \gtrsim 0.5$ the frequency at threshold is always much less than this "standard" value except at the maximum value of k_z/ϵ' available for instability. That this effect is primarily due to departure for quasi-neutrality can be checked by using in (3.4) the

appropriate values of $k^2\lambda^2_{Di}$ at threshold, given below in Eq.(3.6). Eq.(3.4) and the numerical results then agree within about a factor of 2.

Numerical results for the threshold frequency for a Barium plasma are shown in Figs. 1a and 1b. The effects of variation in Θ are illustrated in the latter Figure.

To obtain the threshold, (minimum) density for onset of instability at any k_z/ϵ', we need only insert the solutions of (3.2) in the real part of (3.1). To obtain a marginally-stable solution of (3.1) it is sufficient[11] that $\mathrm{Re}\, H(\omega_0 + i0) \geq 0$, where $\omega_0 = X_0 \Omega_i$ is a solution of (3.2). Thus,

$$k^2\lambda^2_{Di} = -\left(1+\frac{1}{\Theta}\right) - \beta_i \frac{X_0 + X^*/\Theta}{K} Z_r\left(\frac{X_0}{K}\right) - \frac{\beta_e}{\Theta^{3/2}}\sqrt{s}\, Z_r\left(\frac{X_0}{K}\sqrt{\frac{s}{\Theta}}\right) \qquad (3.5)$$

where $Z_r(w)$ denotes the real part of $Z(w)$. ($Z_r(w)$ is negative for positive real w, so we obtain solutions with real density and positive real ω when the final two terms dominate.

In the region of validity of (3.3) the last (electron) term can be neglected altogether, and we have approximately

$$k^2\lambda^2_{Di} \cong \beta_i \frac{X^*}{\Theta K} \left| Z_r\left(\sqrt{\ln\left(\Theta^{1/2}\beta_i/\sqrt{s}\beta_e\right)}\right)\right| - \left(1+\frac{1}{\Theta}\right)$$

or

$$k^2\lambda^2_{Di} \cong \sqrt{\frac{b_i}{2}}\, e^{-b_i} I_0(b_i) \frac{\epsilon'}{k_z} \left| Z_r\left(\sqrt{\ln\left(\Theta^{1/2}\beta_i/\sqrt{s}\beta_e\right)}\right)\right| - \left(1+\frac{1}{\Theta}\right) \qquad (3.6)$$

Note that the threshold density goes to zero as k_z/ϵ' tends to zero, and becomes infinite ($k^2\lambda^2_{Di} \to 0$) when

$$\left.\frac{K_z}{\epsilon'}\right|_{\text{cut-off}} \cong \frac{\sqrt{\frac{b_i}{2}}\, e^{-b_i} I_0(b_i) \left| Z_r\left(\sqrt{\ln\left(\Theta^{1/2}\beta_i/\sqrt{s}\beta_e\right)}\right)\right|}{1+\frac{1}{\Theta}} \qquad (3.7)$$

The approximate threshold equation (3.6) can be regarded either as giving, for each $k_y a_i$, the density for onset of instability for a given k_z/ϵ' or, as in the work of Krall and Rosenbluth, as determining a "critical plasma length" below which instability will not occur for a given mode. In the latter case they identify π/k_z with the plasma length along B.

(To obtain the sufficient condition for stability of Krall and Rosenbluth [10], note that $|Z_r(w)|$ has an absolute maximum of 1.08 at $w \cong 0.9$, that in that case β_i must be very small for moderate θ, and hence $\sqrt{b_i}\beta_i \approx 1/\sqrt{2\pi}$. Then, from (3.6)

$$\left.\frac{\epsilon'}{k_z}\right|_{min} \cong \frac{k^2\lambda_{Di}^2 + (1+\frac{1}{\theta})}{1.08/2\sqrt{\pi}} \cong \frac{10.3}{\pi}\left(k^2\lambda_{Di}^2 + 1 + \frac{T_i}{T_e}\right)$$

This is Krall and Rosenbluth's formula and has been used to determine the dashed curves shown on Figs. 2, 2a and 2b. These curves indeed provide an upper bound on the unstable range of k_z/ϵ' at each density.)

To determine threshold properties for <u>particular</u> modes, (3.6) can be used with fair accuracy for $k_y a_i \gtrsim 0.3$ ($b_i \gtrsim 0.05$). More accurate values, which do not rely on the approximations inherent in (3.3) and (3.6), have been obtained numerically over a more complete range of values of $k_y a_i$; our results are displayed for $\theta = 1$ in Fig. 2 for a proton plasma, and in Fig. 2a for a Barium plasma. The effect of variations in θ (for Ba^+) are indicated in Fig. 2b. It is useful to note that in the regimes for which (3.3) and (3.6) apply both the threshold density and frequency for a given $k_y a_i$ and θ depend only on k_z/ϵ' and it is not necessary to specify $\epsilon' a_i$ as a separate parameter on these curves.

As can be seen in Figs. 2 and 2a, modes with values of $k_y a_i$ 0.4 have <u>two</u> marginally stable "branches" (one

corresponding to the minimum density for onset of instability, the second corresponding to a maximum density (at fixed k_z/ϵ') above which the mode is again stable). These branches have vastly different properties -- this situation arises whenever both solutions of (3.2), for a given $k_z a_i$, yield finite densities from (3.5). On the "low density-low frequency branch" the threshold frequency is given accurately by (3.3) until one approaches the maximum k_z/ϵ' for such modes (Fig.1). On the "high-density branch", on the other hand, the threshold frequency is very well approximated by ω_* (see Fig.1). We consider this case more carefully below (Eq.(3.8)). In a subsequent report we will show that these branches maintain quite different properties in the unstable regime.

The stabilization at high densities of drift modes with low values of $k_y a_i$ (see Figs. 2 and 2a) is an important phenomenon which deserves comment. The stabilization in both the low density and high density regions occurs, of course, because of ion Landau damping overcoming the destabilizing effect on the resonant electrons. However, in the high density regime this comes about not so much because of a decrease in the wave phase speed relative to the ion thermal velocity as because of the fact that ω approaches ω_* more and more closely as $k\lambda_{D_i} \to 0$ at small $k_y a_i$. In that case, the electron density perturbation becomes more and more closely in phase with the potential perturbation, virtually independently of ϵ'/k_z e.

Indeed, in this regime, approximate solutions of (3.2) shows that for marginal stability

$$\omega_0 - \omega_* \cong - \frac{\beta_i \Theta^{3/2}}{\beta_e \sqrt{\delta}} \omega_* \left(1 + \frac{1}{\theta}\right) e^{-\frac{\omega_*^2}{k_z^2 a_i^2}\left(1 - \frac{\delta}{\theta}\right)} \qquad (3.8)$$

(Values of ω_0 closer than this to ω_* lead to stability and vice versa.)

The validity of (3.8) is restricted by the condition

$$\frac{2\beta_i\,\Theta^{3/2}\left(1+\frac{1}{\Theta}\right)}{\sqrt{\delta}\,\beta_e}\,\frac{\omega_*^2}{k_z^2\alpha_i^2}\,e^{-\omega_*^2/k_z^2\alpha_i^2} \ll 1$$

and thus requires $\omega_*/k_z\alpha_i$ greater than about 3 for H^+ and greater than about 3.6 for Ba^+ (cf. Figs. 1 and 1a). Such high phase speeds occur, at threshold, only near the quasi-neutral limit ($k^2\lambda_D^2 \ll 1$) and for small $k_y a_i$. In fact, insertion of (3.8) into (3.5) shows that the real part of the dispersion relation can be satisfied under these conditions only for $k_y a_i$ less than a critical value: with the help of (3.3) we find

$$k_y a_i)_{crit} = 0.44 \tag{3.9}$$

For values of $k_y a_i$ larger than this stabilization cannot occur (at finite densities) by the approach of ω_o to ω_* and requires instead the usual decrease in $\omega/k_z\alpha_i$. This accounts for the essential difference in shape of the stability curves in Figs. 2 - 2b for large and small values of $k_y a_i$.

As can be seen in Figs. 2 - 2b, marginally stable modes with $k_y a_i < k_y a_i)_{crit}$ exhibit a maximum value of k_z/ϵ' at finite densities; as $k^2\lambda_D^2$ decreases below the value corresponding to this maximum (typically, $k^2\lambda_D^2 = 0.1$) the threshold value of k_z/ϵ' also decreases (this is the "high-density branch". From (3.2) it can easily be shown that for $\Theta = 1$

$$\frac{K_{max}^2}{X^2} = \frac{X_*^2 - X^2}{X_* X} \ll 1 \tag{3.10}$$

Combining this result with (3.5), with $\Theta = 1$, we find that

$$\frac{k_z}{\epsilon'}^{max} \cong \frac{k_y a_i}{2}\left(\frac{k_y^2 a_i^2 + k_z\lambda_D^2}{3}\right)^{1/2} \tag{3.11}$$

which agrees very well with the results for $k_y a_i < k_y a_i)_{crit}$ shown on Figs. 2 and 2a.

Unfortunately, because of the limited validity of (3.8) it is quite difficult to give an analytic formula for the shape of the stability curves ($k^2\lambda_D^2$ vs. k_z/ϵ') for values below that corresponding to the maximum k_z/ϵ'. However, we can show that as $k^2\lambda_D^2 \to 0$ there is always a finite minimum k_z/ϵ' for marginal stability. Using (3.5), its value can be determined, in the regime for which (3.8) holds, by the relation (for $\Theta = 1$)

$$\frac{k_z}{\epsilon'}^{min} = \frac{k_z}{\epsilon'}(k^2\lambda_{D_i}^2 \to 0) \simeq \left[k_y^2 a_i^2 - \frac{2}{\sqrt{5}} e^{1/k_y^2 a_i^2}\right]^{1/2} \frac{k_y a_i}{2} < \frac{k_z}{\epsilon'}^{max} \qquad (3.12)$$

which in turn implies $(\omega_* / k_z \alpha_i)^2_{max} = (k_y a_i)^{-2}$ (see Figs. 1 - 1b). Therefore, because of the restriction on (3.8), already mentioned, (3.12) can be used only for $k_y a_i \lesssim 0.28$. Nevertheless, a finite minimum k_z/ϵ' always exists at finite $k_y a_i < k_y a_i)_{crit}$.

Computer results defining the shape of the "high-density branches" of the marginal stability curves for a Barium plasma and for small $k_y a_i$ and $k\lambda_{D_i}$ are shown in Fig.3. These results confirm the behaviour discussed above and enable one to study marginal stability properties near the quasi-neutral limits for small $k_y a_i$. Comparison with Eqs.(3.11) and (3.12) is satisfactory in the regions where the latter apply.

The threshold curves in Figs. 1 - 2b can be used in a variety of ways. To illustrate one possible application, we consider the "Wendelstein II" Stellarator (WII) experiment in Garching. This circular torus has a major diameter of 1 m and contains a Barium plasma with a plasma radius of a few cm and an ion temperature of 2200 ^{o}K. The toroidal magnetic field is 5 kilogauss, and the device operates at measured

densities of from 10^7 cm^{-3} to 10^9 cm^{-3}. Under these conditions, $\Omega_i = 3.5 \times 10^5$ sec^{-1}, while ω_{p_i} varies between 3.5×10^5 and 3.5×10^6 sec^{-1}. At the higher density the mean free path λ_{ei} for collisional electron-ion scattering is approximately 1.5 m, while at the lower density $\lambda_{ei} \approx 100$m. The ion gyro-radius is 1.5 mm. Measured density profiles indicate $(\epsilon')_{max} \cong 1$ cm^{-1}, while the radius at which this maximum occurs lies between 1 cm and 1.5 cm. The temperature is nearly constant in this region. It is clear that collisional effects are important at the higher densities and the present theory would require significant modification for application to that case [1], [3], [19]. For $n = 10^7 - 10^8$ however, the present collisionless theory is applicable. At 10^7, $\Omega_i^2/\omega_{p_i}^2 \doteq 1$, and $\lambda_{D_i}^2 = \frac{1}{2} a_i^2 \frac{\Omega_i}{\omega \rho_i} = 1.12$ mm^2. Because of the way the plasma is created, it is usually assumed that $T_e = T_i$ for the WII experiment.

For these conditions $\epsilon' a_i \doteq 0.15$ and $k_y a_i \doteq 0.1$ "m" (where "m" is the usual cylindrical mode number), insofar as the present slab model can be applied to the stellarator geometry. If we <u>assume</u> that the maximum available wavelength parallel to $\underline{B}$ is determined by the major circumference, then $k_z a_i \doteq 3 \times 10^{-3}$, and $k^z/\epsilon' = 2 \times 10^{-2}$. Then, for an "m = 1" mode, at $n = 10^7$, $2k^2\lambda_{D_i}^2 \doteq 10^{-2}$; for a "m = 3" mode, $2k^2 \lambda_{D_i}^2 = 10^{-1}$; for an "m = 10" mode, $2k^2\lambda_{D_i}^2 = 1.0$, etc. Figs. 1a and 2a then indicate, under the above assumptions, the existence of a large number of unstable drift modes, the properties of which are tabulated (for $n_o = 10^7$ cm^{-3}) in Table (3.1).

Table 3.1 (WII, Ba^+, $n_o = 10^7 cm^{-3}$) $T_e/T_i = 1$

$k_y a_i$	"m"	$2k^2\lambda_{D_i}^2$	Stability	$k_z/\epsilon')_{thresh}$	$\omega)_{thresh}$
0.1	1	10^{-2}	stable	6×10^{-3}	ω_*
0.2	2	4×10^{-2}	unstable	2.5×10^{-2}	ω_*
0.3	3	9×10^{-2}	unstable	4×10^{-2}	ω_*
0.5	5	2.5×10^{-1}	unstable	7×10^{-2}	$k_z\alpha_i\sqrt{\ell n(\beta_i/\sqrt{\delta})}$
1.0	10	1.0	unstable	5.5×10^{-2}	"
↓	↓	↓	↓	↓	↓
3.3	33	10	unstable	2.1×10^{-2}	"
5.0	50	25	stable	1.2×10^{-2}	"
6.0	60	36	stable	9.4×10^{-3}	"
↓	↓	↓	↓	↓	↓

Considerations of this type thus indicate that for this density in the WII Ba^+ plasma, drift-universal modes with "m"-numbers from approximately 2 to 30 would be unstable. At $n_o = 10^8$, assuming we may still neglect collisions, the "m" - 1 and "m" = 2 modes would become stable, while "m" numbers from 3 - 160 would be unstable! Moreover, only for the lowest "m" values (below 5) would the mode be of the type for which $Re(\omega) \cong \omega_*$. For all other unstable modes the real frequency, at least near threshold, is proportional to $k_z\alpha_i$ and generally much less than ω_*. This effect is due largely to strong departure from "quasi-neutrality" (as expected from Eqs. (3.4) and (3.6)) but is also partly due to the fact that $\omega/k_z\alpha_i$ (threshold) is not large, especially if $\theta \lesssim 1$. (The extent to which this latter fact remains true in the unstable regime will be discussed in a later report.) Deviations from these results if $\theta \neq 1$ can be estimated from Figs. 2b and 1b; however, the qualitative conclusions remain unchanged.

Of course, one must have the usual reservations, already noted, concerning the direct applicability in toroidal geometry of results obtained from the simple "slab" model. Our purpose here is primarily to indicate the rather wide range of potentially unstable modes in the collisionless regime, and, further, to point out that the unstable higher m-number modes are unlikely to have frequencies either near ω_* (in the field-free reference frame -- see Section II) or, for that matter, near the more general approximate value given by (3.4). It is our hope that these results might stimulate further research concerning modes of this type, especially with the use of a model more directly applicable to toroidal configurations [16].

References

1 Rukhadse, A.A. and Silin, V.P., "Kinetische Theorie der Drift-Dissipativen Instabilitäten des Plasmas", Lebedev-Institut für Physik, Moskau (1966, in Russian); German translation: IPP Document No. P00617.

2 Rukhadse, A.A. and Silin, V.P., Sov.Physics-Doklady 11, 7, 606 (1967); Translat.from Dokl-Akad.Nauk SSSR, 169, 3, 558 (1966).

3 Hendel, H.W., Coppi, B., Perkins, F., Politzer, P.A., Phys.Rev.Letters 18, 12, 439 (1967); Hendel, H.W., Chu,T.K., Politzer, P.A., Phys.Fluids 11, 11, 2426 (1968).

4 Eastlund, B.J., Josephy, K., Lehery, R.F., Marshal, T.C., Phys.Fluids 9, 12, 2400 (1966).

5 Buchelnikova, M.S., Salimov, R.A., Eidelman, Yu. I., Sov.Phys.JETP 25, 548 (1967); Translated from Zh. eksp. teor. Fiz. 52, 837 (1967).

6 Chen, F.F., Phys. Fluids 8, 912 (1965)

7 Meade, D.M., Phys.Fluids 12, 4, 947 (1969)

8 Rosenbluth, M.N., "Microinstabilities", in Plasma Physics: Lectures Presented at a Seminar, Trieste, p.485, IAEA, Vienna (1965)

9 A sampling of the Russian literature includes: Kadomtsev,B.B., Jour.Nuc.En.Part C (Plasma Physics) 5, 31 (1963); Kadomtsev,B.B., and Timofeev, A.V., Sov.Phys. - Doklady 7, 9, 826 (1963); Rudakov, L.I., and Sagdeev, R.Z., Sov.Phys. JETP 37 (10), 5, 952 (1960); Mikhailovskii, A.B. and Rudakov, L.I., Sov. Phys. JETP 17, 621 (1963). See also: B.B. Kadomtsev, Plasma Turbulence Academic Press, London (1965).

10 Krall,N., and Rosenbluth,M.N., Phys.Fluids 8, 8, 1488 (1965)

11 Callen,J.D., "Absolute and Convective Microinstabilities of a Magnetized Plasma", Ph.D. Thesis, M.I.T. (1968); Also: M.I.T. Center for Space Research Report CSR T 68-3 (1968).

12 Laval,G., Maschke, E.K., Pellat,R., Vuillemin,M., Phys.Rev.Letters 19, 23, 1309 (1967)

13 Saison,R., Plasma Physics 10, 927 (1968)

14 Pearlstein,L.D. and Berk,H.L., Phys.Rev.Letters 23, 5 220 (1969)

15 Politzer, P.A., "Drift Instability in Collisionless Alkali Metal Plasmas", Princeton University Ph.D. Thesis (1969)

16 Rutherford, P.H. and Frieman, E.A., Phys.Fluids 11, 3, 569 (1968)

17 Rutherford, P.H. and Frieman, E.A.,Phys.Fluids 10, 5, 1007 (1967)

18 Fried, B.D. and Conte, S.D., Plasma Dispersion Function, Academic Press, New York (1961)

19 Dupree, T.H., Phys. Fluids 11, 12, 2680 (1968); also: Phys. Fluids 10, 5, 1049 (1967).

Figure Captions

Fig. 1 Frequency at marginal stability for drift modes in a $\theta = 1$, H^+ plasma, as a function of the critical parallel wave number and $k_y a_i$. For sufficiently small $k_y a_i$ there are two "branches" having very different properties; for $k_y a_i$ larger than a critical value (see text) only one "branch" exists. Note the extensive threshold regions for which $\omega / k_z \alpha_i$ is near unity. The analytic formula is Eq.(3.3) of the text.

Fig. 1a Results similar to those in Fig.1, but for a $\theta = 1$, Ba^+ plasma. Because of the heavier ions, $\omega / k_z \alpha_i$ moderately exceeds unity, and Eqs.(3.3) and (3.4) of the text are in fair agreement.

Fig. 1b Illustration of the effects of $\theta = T_e/T_i$ for a Ba^+ plasma.

Fig. 2 Marginal stability curves for a $\theta = 1$, H^+ plasma: threshold and/or cut-off density as a function of k_z/ϵ' and $k_y a_i$. For a given mode the unstable regime is to the left of each curve shown. For $k_y a_i = 0.1$ there are two marginably-stable solutions for values of k_z/ϵ' between 5×10^{-3} and 1.5×10^{-2}. The "high-density" branch for $k_y a_i = 0.1$, at the lower part of the figure, corresponds to the upper frequency branch in Fig.1. For values of $k_y a_i$ 0.5 only one marginally stable solution exists at each k_z/ϵ' (see text).

Fig. 2a Results similar to those in Fig.2, but for a $\theta = 1$ Ba^+ plasma.

Fig. 2b Illustration of the effects of $\theta = T_e/Ti$ on the marginal stability curves for a Ba^+ plasma.

Fig.3 Extension to small values of $k^2\lambda_{D_i}^2$ of the "high density" branches of the marginal stability curves for a $\Theta = 1$, Ba^+ plasma.

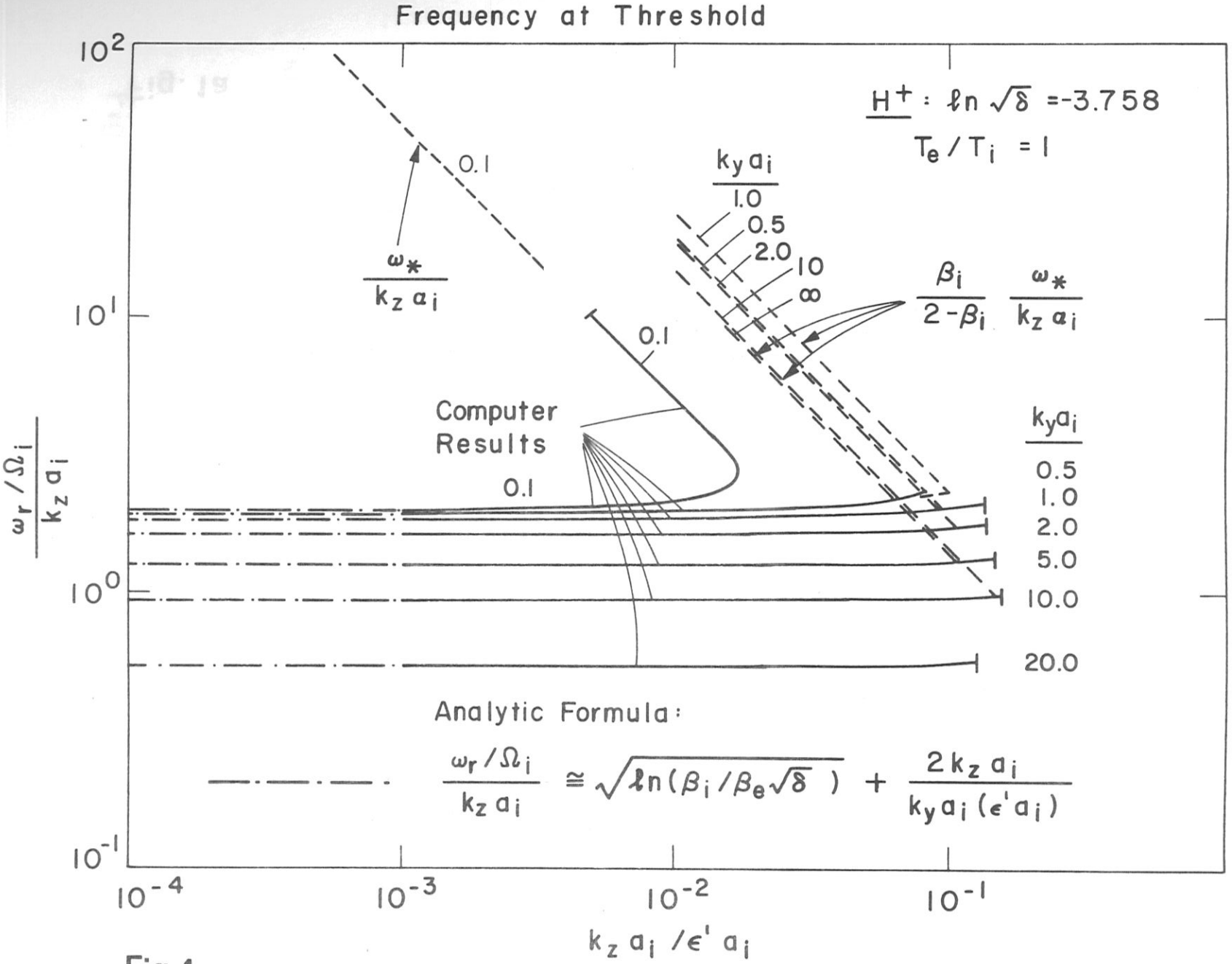
Frequency at Threshold
H^+ : $\ell n \sqrt{\delta}$ = -3.758
T_e / T_i = 1
$k_y a_i$
1.0
0.5
2.0
10
∞
0.1
$\frac{\omega_*}{k_z a_i}$
$\frac{\beta_i}{2-\beta_i}$ $\frac{\omega_*}{k_z a_i}$
Computer Results
0.1
0.1
$k_y a_i$
0.5
1.0
2.0
5.0
10.0
20.0
$\frac{\omega_r / \Omega_i}{k_z a_i}$
10^2
10^1
10^0
10^{-1}
10^{-4}
10^{-3}
10^{-2}
10^{-1}
$k_z a_i / \epsilon' a_i$
Analytic Formula:
$\frac{\omega_r / \Omega_i}{k_z a_i} \cong \sqrt{\ell n (\beta_i / \beta_e \sqrt{\delta})} + \frac{2 k_z a_i}{k_y a_i (\epsilon' a_i)}$

Fig. 1

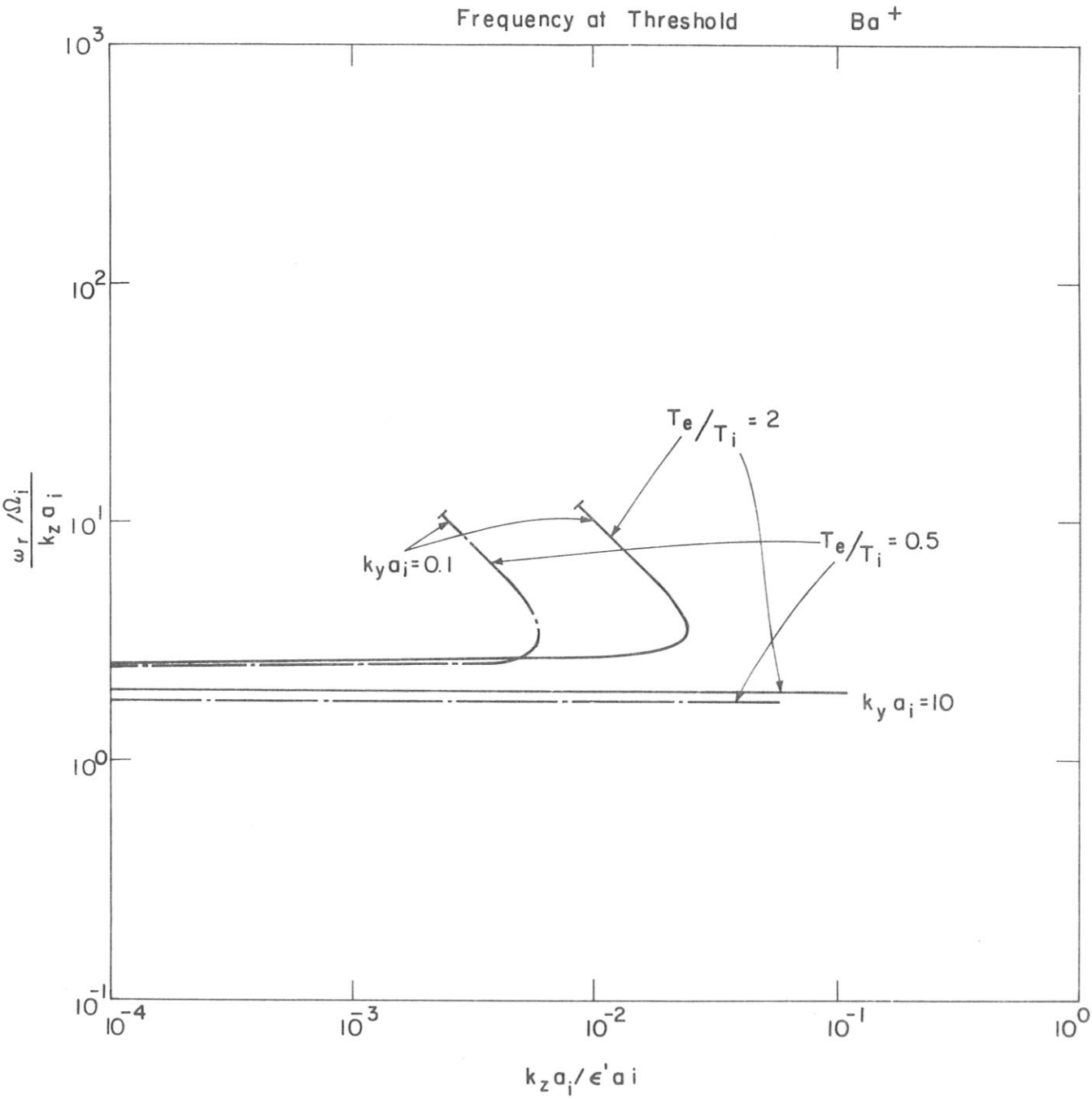
Frequency at Threshold
Ba +
10^3
10^2
10^1
10^0
10^{-1}
$\frac{\omega_r / \Omega_i}{k_z a_i}$
$T_e/T_i = 2$
$T_e/T_i = 0.5$
$k_y a_i = 0.1$
$k_y a_i = 10$
10^{-4}
10^{-3}
10^{-2}
10^{-1}
10^0
$k_z a_i / \epsilon' a_i$

Fig. 1b

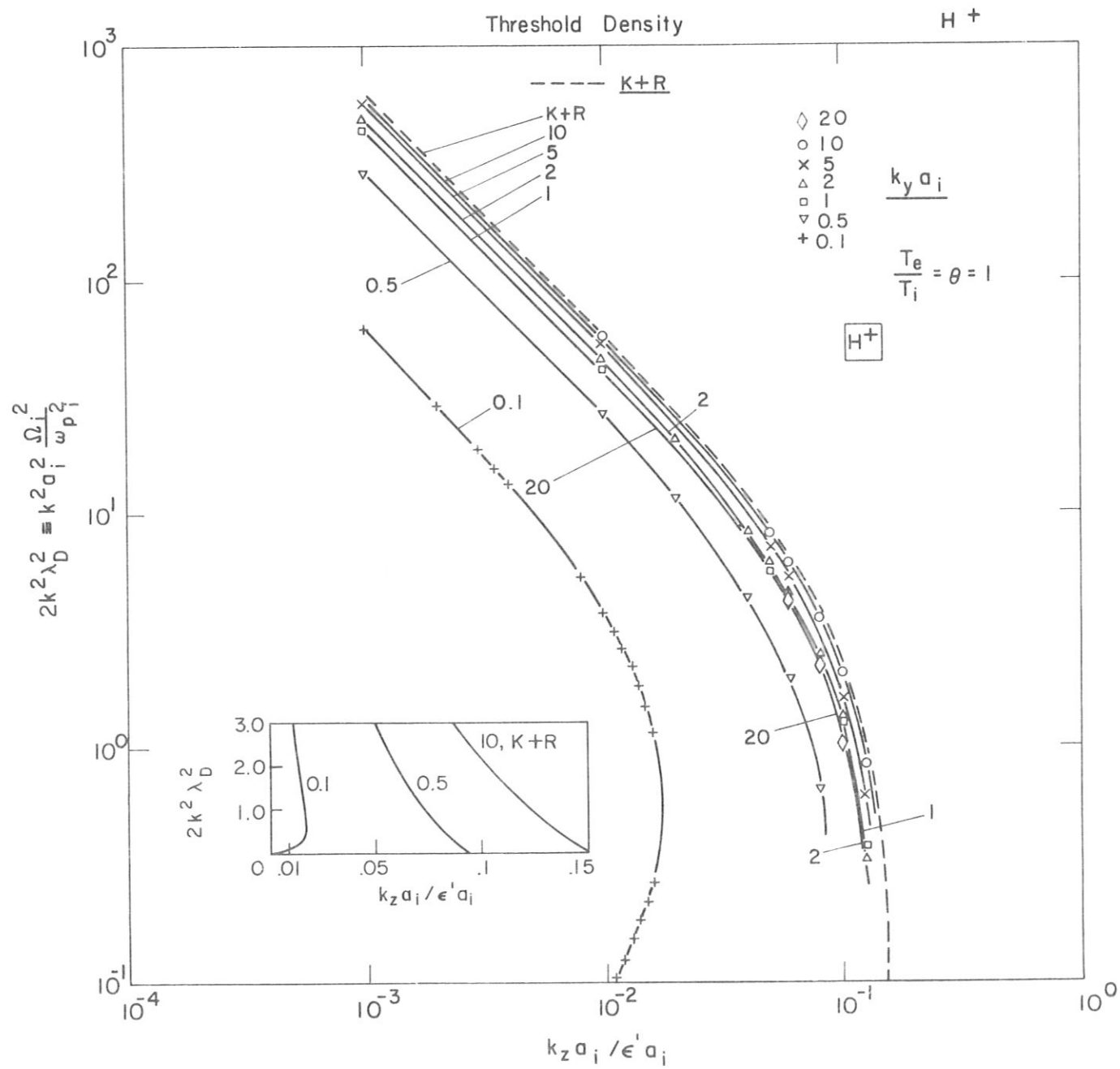
Threshold Density
H +
K+R
$k_y a_i$
$\frac{T_e}{T_i} = \theta = 1$
H+
$2k^2\lambda_D^2 \equiv k^2 a_i^2 \frac{\Omega_i^2}{\omega_{pi}^2}$
$k_z a_i / \epsilon' a_i$
$2k^2\lambda_D^2$
10, K+R
0.1
0.5

Fig. 2

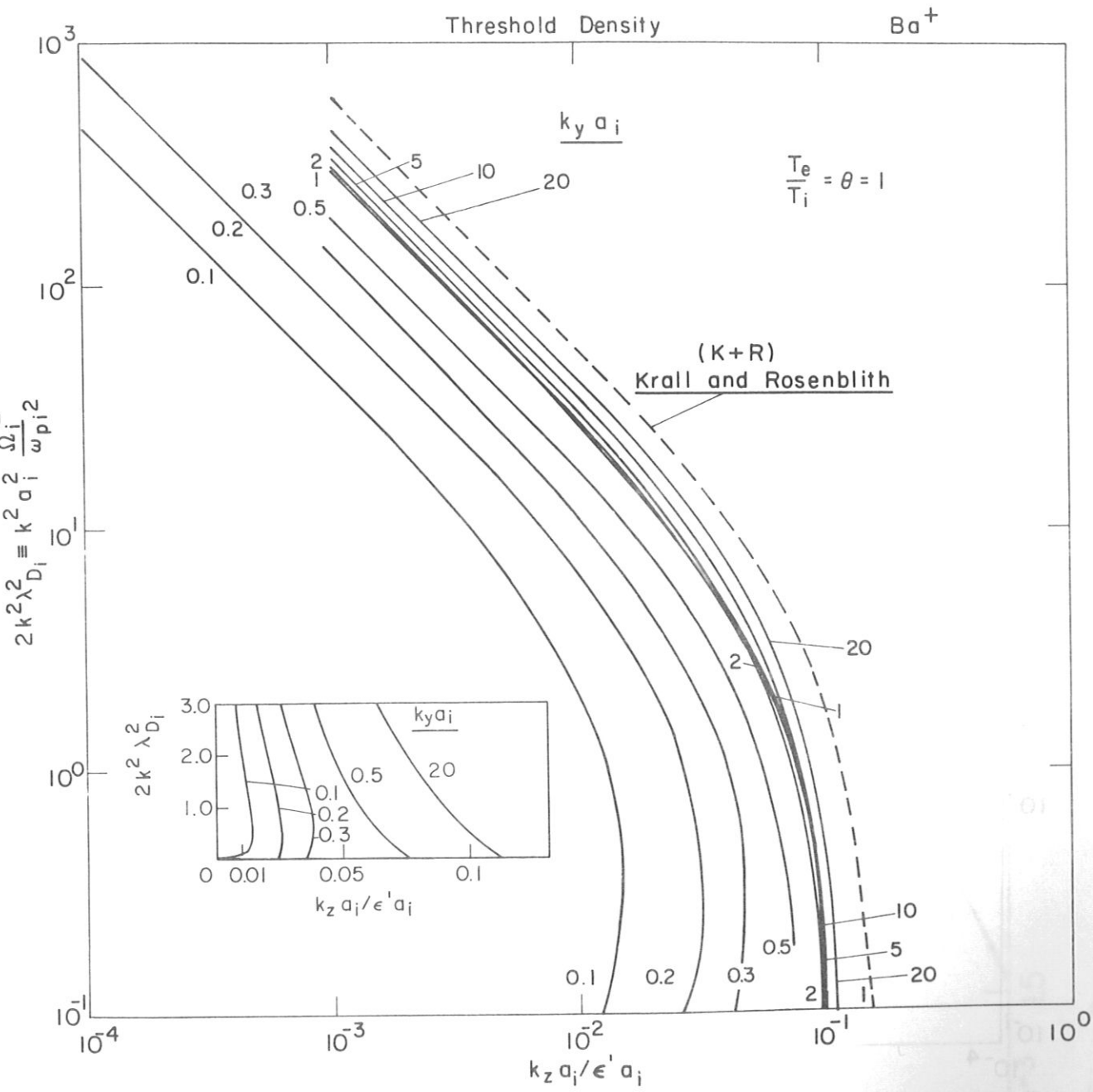
Threshold Density
Ba+
$k_y a_i$
$\frac{T_e}{T_i} = \theta = 1$
(K+R)
Krall and Rosenblith
$2k^2\lambda_{D_i}^2 \equiv k^2 a_i^2 \frac{\Omega_i^2}{\omega_{pi}^2}$
$k_z a_i/\epsilon' a_i$
$2k^2\lambda_{D_i}^2$
$k_y a_i$
$k_z a_i/\epsilon' a_i$

Fig. 2a

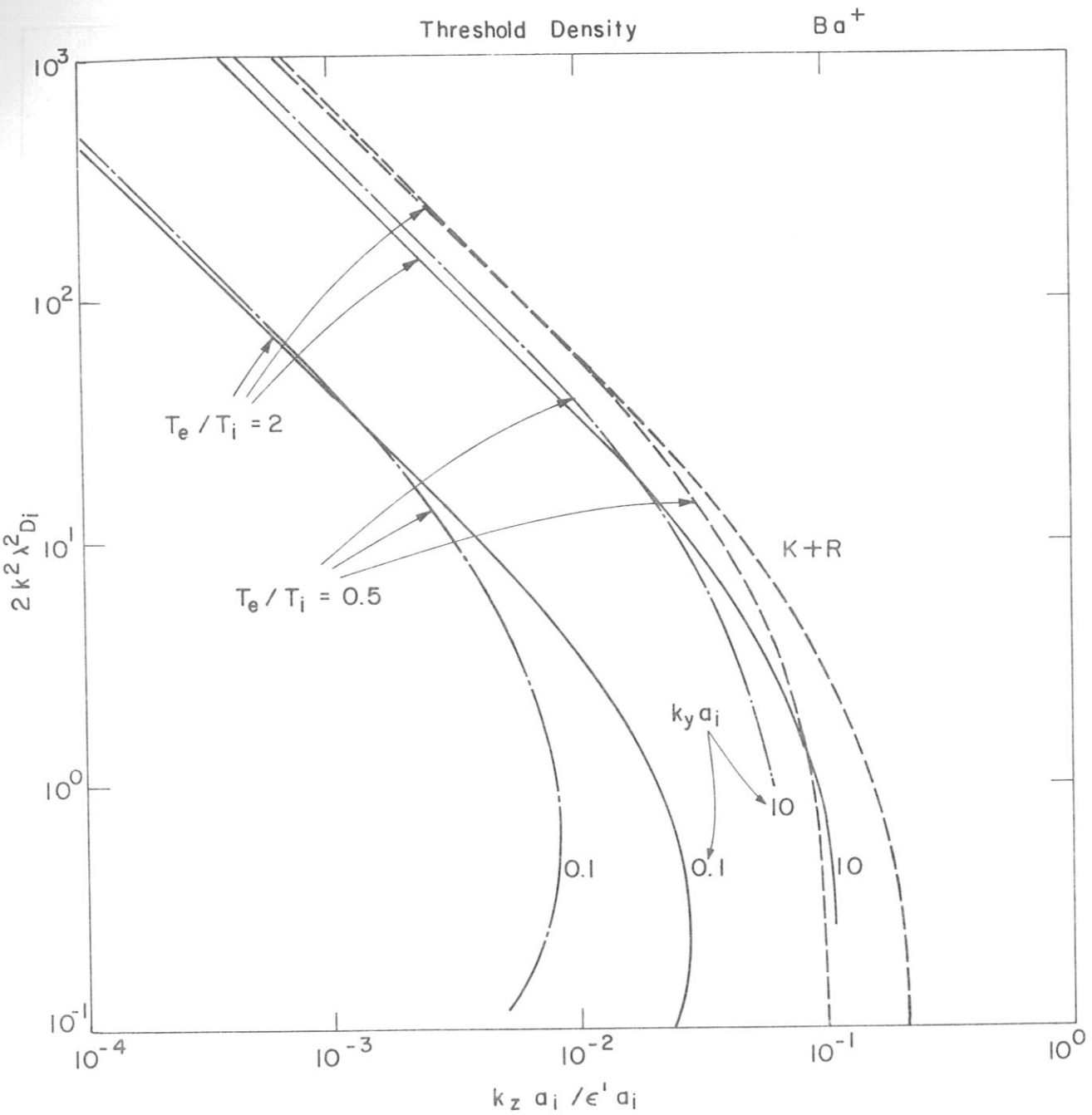
Threshold Density
Ba+
10^3
10^2
10^1
10^0
10^{-1}
$2k^2\lambda^2_{Di}$
$T_e / T_i = 2$
$T_e / T_i = 0.5$
K+R
$k_y a_i$
10
0.1
0.1
10
10^{-4}
10^{-3}
10^{-2}
10^{-1}
10^0
$k_z a_i / \epsilon' a_i$

Fig. 2b

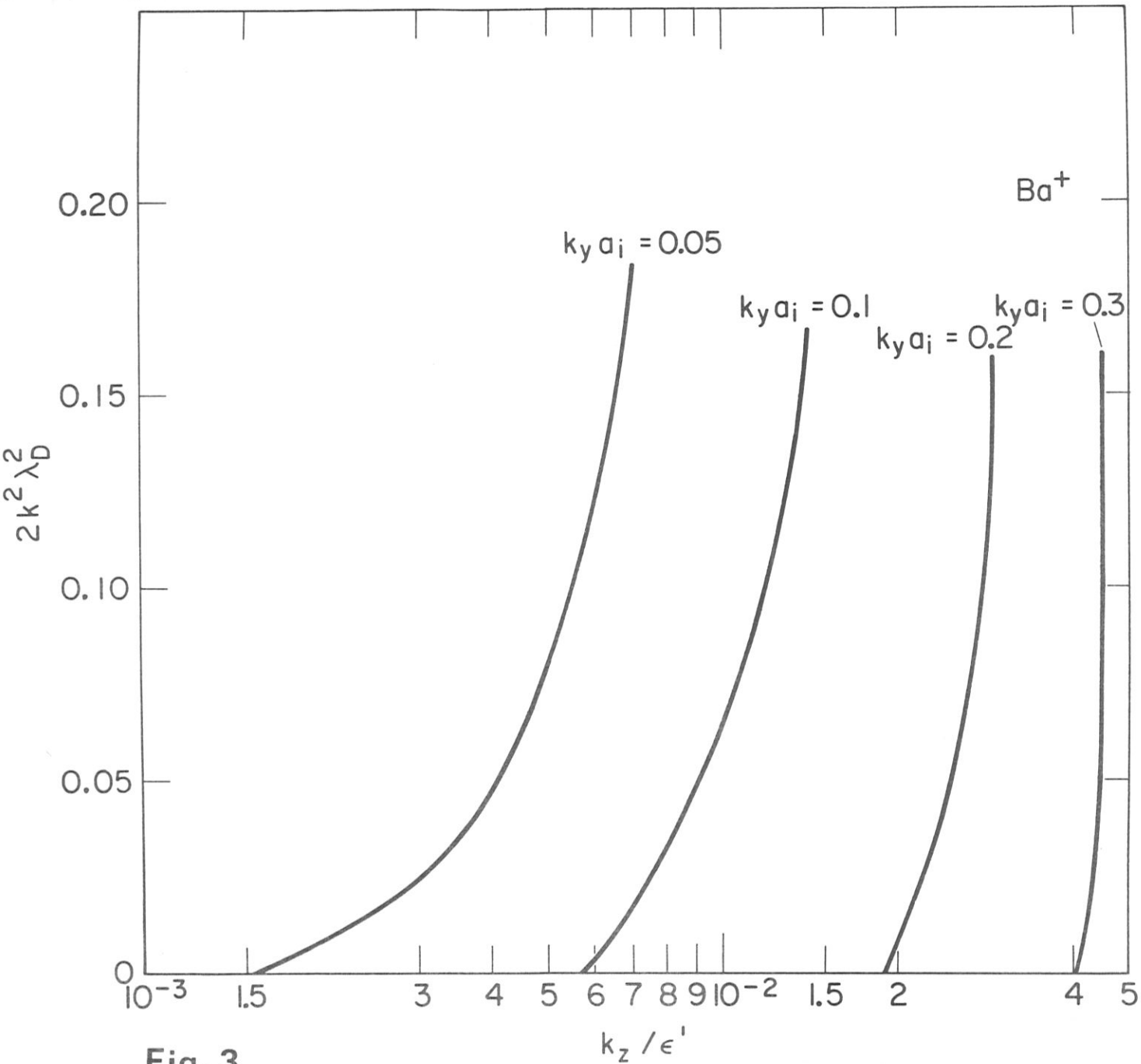
Ba+
$k_y a_i = 0.05$
$k_y a_i = 0.1$
$k_y a_i = 0.2$
$k_y a_i = 0.3$
0.20
0.15
0.10
0.05
0
$2k^2\lambda_D^2$
10^{-3}
1.5
3
4
5
6
7
8
9
10^{-2}
1.5
2
4
5
k_z/ϵ'

Fig. 3